

Exact equivalent-profile formulation for bent optical waveguides

D M Shyrok

Department of Communications, Optics and Materials, Technical University of Denmark, Building 343v, 2800 Kgs. Lyngby, Denmark

E-mail: ds@com.dtu.dk

Abstract. A widespread, intuitive and computationally inexpensive method to analyze light guidance through waveguide bends is by introducing an equivalent straight waveguide with refractive index profile modified to account for actual waveguide bend. Here we revise the commonly used equivalent-index formula, ending up with its simple extension that enables rigorous treatment of one- and two-dimensionally confined, uniformly bent waveguides, including tightly coiled microstructure fibers, curved ridge waveguides and ring microresonators. We also show that such technique is applicable only to waveguides composed of isotropic or uniaxially anisotropic materials, with anisotropy axis directed perpendicular to the curvature plane.

To understand and to predict light wave behavior at waveguide bends was of major importance and interest to integrated- and fibre-optics community from around 1970s and onwards. Today this interest is stimulated largely by two developments: (i) increasing the packaging density of integrated-optic circuits, backed by minimizing integrated waveguide bend radii while keeping bend losses at a tolerable level; and (ii) the advent of photonic crystal fibers possessing quite complicated, high index-contrast dielectric profiles as compared to step- or graded-index fibers for which early theoretical methods to treat bend losses were developed.

Numerical methods to simulate light propagation through waveguide bends, such as beam propagation method [1], the method of lines [2, 3], as well as more general-purpose finite-element and finite-difference techniques, can be very demanding computationally: in one recent example [4], a 64-processors cluster was used in full-vector finite-element modelling. No wonder one leans to analytic techniques to reduce computation burden whenever possible; one such technique, perhaps the simplest and most widely used in modelling of microstructure fibre bends today [5, 6, 7, 8], is equivalent-profile method [9, 10]. It reduces dimensionality of the problem by replacing actual waveguide bend by a straight piece with refractive index profile

$$n^2 = \epsilon_C(1 + y/R)^2 \approx \epsilon_C(1 + 2y/R), \quad (1)$$

where ϵ_C is dielectric permittivity in the bent waveguide cross-section, as measured in Cartesian frame, R is the bend radius pointing from the x -directed curvature axis

to a (somewhat arbitrary) waveguide central plane, y the distance from that plane. Designed for elegant and inexpensive treatment of bends, though, formula (1) grounds on approximations whose validity may often be questioned, as those of weak-guidance regime and small curvature ($y/R \ll 1$), and originally was introduced for quite a specific case of non-magnetic, step-index, low index-contrast fibre. In this Letter we overcome all these limitations by an alternative, first-principle derivation of expressions for modified dielectric permittivity ϵ and magnetic permeability μ analogous to (1), but applicable to waveguides of arbitrary cross-section under the only assumption that bend radius is constant (while not necessarily large).

Following Schouten [11] and Post [12], we start from the generally covariant Maxwell equations

$$2\partial_{[\lambda}E_{\nu]} = -\dot{B}_{\lambda\nu}, \quad \partial_{[\kappa}B_{\lambda\nu]} = 0, \quad (2)$$

$$\partial_{\nu}\mathfrak{H}^{\lambda\nu} = \dot{\mathfrak{D}}^{\lambda} + \mathfrak{j}^{\lambda}, \quad \partial_{\lambda}\mathfrak{D}^{\lambda} = \rho. \quad (3)$$

Here the square brackets denote alternation: $\cdot_{[\lambda\nu]} = \frac{1}{2!}(\cdot_{\lambda\nu} - \cdot_{\nu\lambda})$, E_{λ} and $B_{\lambda\nu} = -B_{\nu\lambda}$ are covariant electric vector and magnetic bivector fields coinciding with electric and magnetic three-vectors \mathbf{E} and \mathbf{B} in Cartesian frame, $\mathfrak{H}^{\lambda\nu} = -\mathfrak{H}^{\nu\lambda}$ and \mathfrak{D}^{λ} are contravariant magnetic bivector density and electric vector density of weight +1 corresponding to \mathbf{H} and \mathbf{D} , \mathfrak{j}^{λ} and ρ are electric current and charge densities, $\lambda, \nu = 1 \dots 3$. With such transformation characteristics assigned to the electromagnetic field quantities, Eqs. (2), (3) are known to be form-invariant [11, 12], i.e., they do not change their form under arbitrary revertible coordinate transformations. It might be practical to convert Eqs. (2), (3) with use of dual equivalents $\tilde{\mathfrak{B}}^{\kappa} = \frac{1}{2}\tilde{\mathfrak{e}}^{\kappa\lambda\nu}B_{\lambda\nu}$ and $\tilde{H}_{\kappa} = \frac{1}{2}\tilde{\mathfrak{e}}_{\kappa\lambda\nu}\mathfrak{H}^{\lambda\nu}$, where $\tilde{\mathfrak{e}}^{\kappa\lambda\nu}$ and $\tilde{\mathfrak{e}}_{\kappa\lambda\nu}$ are pseudo (hence tildes) permutation fields equal to Levi-Civita symbol in any coordinate system, to the form directly reminiscent of Maxwell equations in Cartesian frame:

$$\tilde{\mathfrak{e}}^{\kappa\lambda\nu}\partial_{\lambda}E_{\nu} = -\mu^{\kappa\lambda}\dot{H}_{\lambda}, \quad \partial_{\kappa}\mu^{\kappa\lambda}\tilde{H}_{\lambda} = 0, \quad (4)$$

$$\tilde{\mathfrak{e}}^{\kappa\lambda\nu}\partial_{\lambda}\tilde{H}_{\nu} = \epsilon^{\kappa\lambda}\dot{E}_{\lambda} + \mathfrak{j}^{\kappa}, \quad \partial_{\kappa}\epsilon^{\kappa\lambda}E_{\lambda} = \rho, \quad (5)$$

while the constitutive relations are implied being

$$\tilde{\mathfrak{B}}^{\lambda} = \mu^{\lambda\nu}\tilde{H}_{\nu}, \quad \mathfrak{D}^{\lambda} = \epsilon^{\lambda\nu}E_{\nu}. \quad (6)$$

Here $\epsilon^{\lambda\nu}$ and $\mu^{\lambda\nu}$ are tensor densities of weight +1:

$$\epsilon^{\lambda\nu} = |\Delta|^{-1}J_{\lambda'}^{\lambda}J_{\nu'}^{\nu}\epsilon^{\lambda'\nu'}, \quad \mu^{\lambda\nu} = |\Delta|^{-1}J_{\lambda'}^{\lambda}J_{\nu'}^{\nu}\mu^{\lambda'\nu'}, \quad (7)$$

as stipulated by transformation characteristics of the fields \tilde{H}_{λ} , $\tilde{\mathfrak{B}}^{\lambda}$, E_{λ} and \mathfrak{D}^{λ} . We denote by $J_{\lambda'}^{\lambda} \equiv \partial_{\lambda'}x^{\lambda}$ the Jacobian transformation matrix, and $\Delta \equiv \det J_{\lambda'}^{\lambda}$ its determinant. In this formulation, geometry enters Maxwell equations (4), (5) through material fields (7) exclusively; since the form of (4), (5) is precisely as if they were written in Cartesian components, a multitude of analytic and numeric methods developed for rectangular Cartesian frame apply. Furthermore, whenever $\epsilon^{\lambda\nu}$ and $\mu^{\lambda\nu}$ happen to be independent of one (or more) of the coordinates in a chosen coordinate system, that coordinate (or those coordinates) can be separated in the usual manner, like z

coordinate in the case of straight homogeneous waveguide. Now we show that in cylindrical coordinates $\{x, r, \phi\}$, such ruling out of angular coordinate ϕ is the case for, in particular, isotropic guide of arbitrary cross-section, bent along ϕ , and specify Eqs. (7) for that case.

Since isotropic media are defined as those possessing scalar (though, in general, position-dependent) permittivity ϵ_C and permeability μ_C , as referred to Cartesian system, transformation rules (7) reduce to

$$\epsilon^{\lambda\nu} = g^{-\frac{1}{2}} g^{\lambda\nu} \epsilon_C, \quad \mu^{\lambda\nu} = g^{-\frac{1}{2}} g^{\lambda\nu} \mu_C, \quad (8)$$

owing to transformation behavior of the fundamental (metric) tensor $g^{\lambda\nu} = J_{\lambda'}^{\lambda} J_{\nu'}^{\nu} g^{\lambda'\nu'}$; its determinant $g \equiv \det g^{\lambda\nu} = \det^2 J_{\lambda'}^{\lambda}$ insofar as $\det g^{\lambda'\nu'} = 1$ in Cartesian frame. Equations (8) resemble ‘effective’ permittivity and permeability introduced in [13], albeit we would refrain from using the word ‘effective’, on the ground that (8) are nothing but transformation rules for the permittivity and permeability of isotropic media. With transformation from orthogonal Cartesian to cylindrical coordinates given by

$$x = x, \quad y = r \cos \phi, \quad z = r \sin \phi. \quad (9)$$

(x defines bending axis), one can find the Cartesian-to-cylindrical transformation matrix for contravariant components

$$J_{\lambda'}^{\lambda} = \begin{pmatrix} 1 & 0 & 0 \\ 0 & \cos \phi & \sin \phi \\ 0 & -r^{-1} \sin \phi & r^{-1} \cos \phi \end{pmatrix} \quad (10)$$

and contravariant metric tensor

$$g^{\lambda\nu} = \begin{pmatrix} 1 & 0 & 0 \\ 0 & 1 & 0 \\ 0 & 0 & r^{-2} \end{pmatrix}, \quad (11)$$

$g^{-\frac{1}{2}} = r$. After substituting these expressions in Eqs. (8), separating the ϕ variable in Maxwell equations (4), (5) and differentiating the $\exp(i\beta\phi)$ multipliers with respect to ϕ , normalizing the propagation constant β by R in the usual manner and introducing shifted coordinate $y = r - R$, one obtains

$$\epsilon_{xx} = \epsilon_{yy} = \epsilon_C(1 + y/R), \quad \epsilon_{zz} = \epsilon_C(1 + y/R)^{-1} \quad (12)$$

(we do not distinguish between co- and contravariant indices once particular coordinate system is chosen), and similarly for permeability components:

$$\mu_{xx} = \mu_{yy} = \mu_C(1 + y/R), \quad \mu_{zz} = \mu_C(1 + y/R)^{-1}. \quad (13)$$

Note that expressions for ϵ_{xx} and ϵ_{yy} , multiplied by their magnetic counterparts, lead to refractive tensor components $n_{xx}^2 = \epsilon_{xx}\mu_{xx}$ and $n_{yy}^2 = \epsilon_{yy}\mu_{yy}$ precisely in line with standard formula (1) in the case of non-magnetic media. The ϵ_{zz} and μ_{zz} components manifestly differ from the rest, however (see figure 1); this difference becomes especially pronounced when departing from weakly guiding approximation, as soon as non-negligible z -components of electric and magnetic fields would ‘probe’ the $\epsilon_{zz}(x, y)$ and $\mu_{zz}(x, y)$ profiles then.

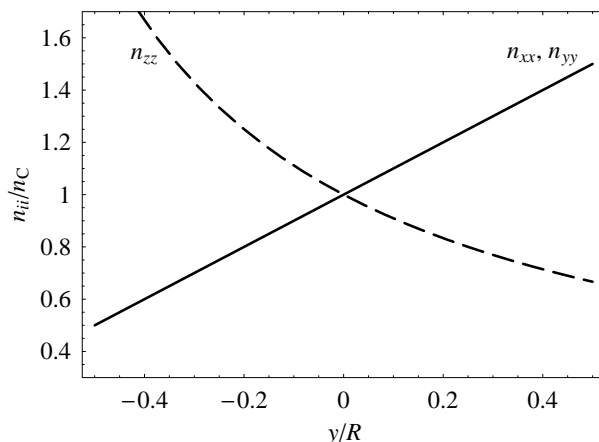


Figure 1. Departure from refractive index n_C of waveguide with bending, for diagonal refractive tensor components $n_{ii} = \sqrt{\epsilon_{ii}\mu_{ii}}$ according to Eqs. (12), (13).

A benchmark example to illustrate the validity of formulae (12), (13) is a problem of light propagation through a homogeneous slab waveguide bend that permits precise analytic treatment—see e.g. [14] for an overview. In our approach, covariant Maxwell curl equations, $\tilde{\mathfrak{E}}^{\kappa\lambda\nu}\partial_\lambda E_\nu = -\mu^{\kappa\lambda}\dot{\tilde{H}}_\lambda$ and $\tilde{\mathfrak{E}}^{\kappa\lambda\nu}\partial_\lambda \tilde{H}_\nu = \epsilon^{\kappa\lambda}\dot{E}_\lambda$, reduce to four independent first-order scalar equations then, grouped in two pairs: one for the E_x , \tilde{H}_ϕ components (TE mode):

$$\partial_r E_x = ik \frac{\mu_C}{r} \tilde{H}_\phi, \quad (14)$$

$$\partial_r \tilde{H}_\phi = ik \left(\epsilon_C r - \frac{n_{\text{eff}}^2 R^2}{\mu_C r} \right) E_x, \quad (15)$$

where k is the free-space wavenumber, $n_{\text{eff}} = \beta/(kR)$ the dimensionless mode index; and another pair for E_ϕ , \tilde{H}_x (TM mode). To derive second-order equation for E_x (which can be regarded as an eigenproblem in n_{eff}), we differentiate (14) with respect to r , use (15) for $\partial_r \tilde{H}_\phi$ and $ik\tilde{H}_\phi = \frac{r}{\mu_C}\partial_r E_x$ to exclude \tilde{H}_ϕ . This leads, in the regions of constant μ_C , to

$$\frac{\partial^2 E_x}{\partial r^2} + \frac{1}{r} \frac{\partial E_x}{\partial r} + k^2 \left(\epsilon_C \mu_C - \frac{n_{\text{eff}}^2 R^2}{r^2} \right) E_x = 0, \quad (16)$$

a Bessel equation used customarily in exact analysis of bent slab waveguides [14, 15], while an attempt to get similar equation with use of approximate equivalent-index formula (1) fails. The results of full-vector two-dimensional finite-difference frequency-domain (FDFD) modelling of confined modes in a high-contrast step-index optical fibre (figure 2) demonstrate systematic discrepancy between approximate model (1) and formulae (12), (13); a discrepancy which can not be tolerated in realistic simulations of high index contrast ridge waveguides and holey fibers, ring microresonators, or sharp fibre bends such as those due to non-perfect alignment of fibre splices.

A closer inspection of (10) brings to conclusion that the only type of initial anisotropy in ϵ_C and μ_C which still permits ruling out the ϕ dependence in $\epsilon^{\lambda\nu}$ and $\mu^{\lambda\nu}$

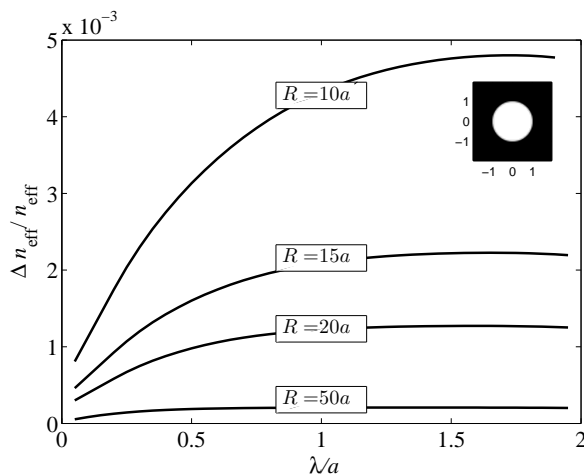


Figure 2. The difference in fundamental mode indices at various bend radii R of a step-index fibre of radius a and dielectric index $n_{\text{core}} = 1.45$ in the air background, calculated numerically with (1) and (12), (13).

transformed according to (7) is that of uniaxial crystal with anisotropy axis pointing in the x direction (i.e., along the bend axis):

$$\epsilon_{\text{C}} = \begin{pmatrix} \epsilon_b & 0 & 0 \\ 0 & \epsilon_a & 0 \\ 0 & 0 & \epsilon_a \end{pmatrix}. \quad (17)$$

In that case, one gets instead of formulae (12):

$$\epsilon_{xx} = \epsilon_b(1 + y/R), \quad (18)$$

$$\epsilon_{yy} = \epsilon_a(1 + y/R), \quad (19)$$

$$\epsilon_{zz} = \epsilon_a(1 + y/R)^{-1}, \quad (20)$$

and likewise for modified μ . Unfortunately, however, the case of anisotropy given by (17) is not one encountered when modelling, e.g., photonic bandgap fibre filled with liquid crystal; for that and other examples of curved waveguides possessing anisotropy of some general kind, *rigorous* equivalent-profile formulation is not applicable and should be substantiated by more brute-force numeric or less stringent analytic techniques.

In summary, equivalent-profile expressions (12), (13) to treat waveguide bends have been presented. Unlike conventional formula (1), they hold for arbitrarily tight bends, arbitrary high-contrast material profiles, and permit the inclusion of magnetic parts. This offers three-dimensional modelling accuracy with those existing full-vectorial two-dimensional finite-difference or finite-element solvers which permit 3×3 diagonal matrices for ϵ and μ be put in. Eliminating the restraints on bend radius and refractive index contrast enables one to simulate also the whispering-gallery modes in spherical, toroidal and other types of optical microcavities. The principal limitation of the equivalent-profile technique is that many cases of non-trivial anisotropy can not be treated rigorously in the manner above.

References

- [1] M. Rivera, *J. Lightwave Technol.* **13**, 233 (1995).
- [2] R. Pregla, *J. Lightwave Technol.* **14**, 634 (1996).
- [3] I. A. Goncharenko, S. F. Helfert, and R. Pregla, *Int. J. Electron. Commun.* **59**, 185 (2005).
- [4] J. Koning, R. N. Rieben, and G. H. Rodrigue, *J. Lightwave Technol.* **23**, 4147 (2005).
- [5] J. C. Baggett, T. M. Monro, K. Furusawa, V. Finazzi, and D. J. Richardson, *Opt. Commun.* **227**, 317 (2003).
- [6] A. Argyros, T. A. Birks, S. G. Leon-Saval, C. M. B. Cordeiro, and P. St. J. Russell, *Opt. Express* **13**, 2503 (2005).
- [7] Y. Tsuchida, K. Saitoh, and M. Koshiba, *Opt. Express* **13**, 4770 (2005).
- [8] J. M. Fini, *Opt. Express* **14**, 69 (2006).
- [9] D. Marcuse, *J. Opt. Soc. Am.* **66**, 311 (1976).
- [10] D. Marcuse, *Appl. Opt.* **21**, 4208 (1982).
- [11] J. A. Schouten, *Tensor Analysis for Physicists* (Clarendon, Oxford, 1951).
- [12] E. J. Post, *Formal Structure of Electromagnetics* (North-Holland, Amsterdam, 1962).
- [13] A. J. Ward and J. B. Pendry, *J. Modern Opt.* **43**, 773 (1996).
- [14] K. R. Hiremath, M. Hammer, R. Stoffer, L. Prkna, and J. Čtyroký, *Opt. Quantum Electron.* **37**, 37 (2005).
- [15] R. Jedidi and R. Pierre, *J. Lightwave Technol.* **23**, 2278 (2005).